INSTITUT DE FRANCE
Académie des sciences

Comptes Rendus

Mécanique

Matei Badalan, Lucie Adisson, Arthur Boldron, Jean-Luc Achard, Giovanni Ghigliotti, Guillaume Balarac and Frédéric Bottausci

A Soft Landing Approach for the Centrifugal Microgel Synthesis Process

Volume 351 (2023), p. 83-103

Published online: 27 February 2023

https://doi.org/10.5802/crmeca.154

This article is licensed under the
Creative Commons Attribution 4.0 International License.
http://creativecommons.org/licenses/by/4.0/

Les Comptes Rendus. Mécanique *sont membres du Centre Mersenne pour l'édition scientifique ouverte*
www.centre-mersenne.org
e-ISSN : 1873-7234

Comptes Rendus
Mécanique
2023, Vol. 351, p. 83-103
https://doi.org/10.5802/crmeca.154

Spontaneous articles / *Articles spontanés*

A Soft Landing Approach for the Centrifugal Microgel Synthesis Process

Matei Badalan [a, b], Lucie Adisson [a], Arthur Boldron [a], Jean-Luc Achard [a, b], Giovanni Ghigliotti [b], Guillaume Balarac [b] and Frédéric Bottausci [*, a]

[a] Univ. Grenoble Alpes, CEA, LETI, Technologies for Healthcare and biology division, Microfluidic Systems and Bioengineering Lab, 38000 Grenoble, France

[b] Univ. Grenoble Alpes, CNRS, Grenoble INP, LEGI, 38000 Grenoble, France

E-mail: frederic.bottausci@cea.fr (F. Bottausci)

Abstract. Centrifugal microencapsulation has been shown to be a promising encapsulation technique, satisfying at the same time many requirements needed for biomedical applications (monodispersity, controlled size, spherical shape, sterile production environment) and allowing a high capsules production rate, using only conventional lab material. Another important advantage of this technology is the ability to process highly viscous biopolymer solutions. The usage of such solutions is desirable in multiple biomedical applications, because they yield capsules with improved mechanical properties (stiffness and yield strength) and with optimised porosity, which increases the immunoprotection in the case of biomaterial encapsulation applied to cell therapy and enhances a prolonged dissolution behaviour in the case of drug delivery applications. However, previous studies have shown that spherical capsules cannot be obtained using highly viscous solutions, and a capsule tail is always present when such solutions are used. This represents a significant limitation of this technology, since capsule shape regularity is an important requirement for various biomedical applications (e.g. cell therapy implants, drug delivery). In this article we propose and validate experimentally an adaptation of the centrifugal microencapsulation, based on the concept of "soft landing" [1]. This technique allows the production of ellipsoidal and spherical capsules using very viscous (typically up to several tens of $Pa.s$) biopolymer solutions.

Keywords. Alginate microcapsules, Centrifugal microfluidics, Microencapsulation, Shape optimisation, High viscosity.

Note. M. Badalan and L. Adisson contributed equally to this work.

Manuscript received 13 July 2022, revised and accepted 22 November 2022.

[*] Corresponding author.

1. Introduction

Centrifugal alginate hydrogel synthesis has been proven to be a promising technique for microencapsulation and microbead generation, and has been successfully employed for producing monodisperse Calcium-alginate particles with controlled size and shape for a large range of applications (microcarriers, encapsulation, self-assembly, etc.) [2, 3]. In the last decade, various teams have worked to improve the design and optimise the performances of centrifugal microparticle generation devices [2, 4–18], while proving different examples of successful application in different fields, in particular biological and biomedical. Other studies have been dedicated to the generalisation of the usage of this technology by establishing generic phase diagrams [3], to the experimental and theoretical analysis and description of certain stages of the microgels generation process [19–22], or to the complete description of all the transformation steps involved in the process [23].

Centrifugal encapsulation stands out from other external gelation encapsulation techniques by its ability to process highly viscous polymer solutions while using only common lab material. For other encapsulation methods, processing highly viscous solutions is either impossible or requires very specialised equipment, while losing some of the other qualities of the encapsulation process (sterility, controlled environment and temperature, beads monodispersity in size and shape, etc.) [24]. Capsules obtained from highly concentrated (and thus viscous) polymer solutions present certain advantages for different applications in the biomedical field: (i) increased mechanical resistance, stability and stiffness [25–27], which are important to control in implant applications [28]; (ii) smaller pore sizes, which increases the immunoprotection in the case of cell therapy applications [29]; (iii) an extended dissolution behaviour in the case of drug release applications [24, 30, 31].

In addition to the advantages of using highly viscous solutions, a spherical shape of the capsules is desired in many biomedical applications (e.g. implant, drug delivery, cell therapy) due to a better diffusion capacity (high surface area to volume ratio), a high resistance to mechanical stress, a short and uniform diffusion time, a more fluent transport inside tubing, while offering access to a number of implantation sites by a simple injection procedure [32–38]. The presence of a protuberance involves that capsule surface is not regular and not smooth, which can lead, for instance in the case of implant applications, to the failure of the implant function [39–41].

An important observation from the literature is that several authors, using slightly different centrifugal devices, have reported that fabrication of spherical or ellipsoidal capsules is not possible for alginate solutions with a concentration above a certain threshold which often lies around 2% w/v [2, 18]. In previous work, it has been shown that capsules formed using alginate solutions with high concentrations always present a protuberance[1] (see Figure 1) [3, 23]. The existence of an upper limit in alginate concentration (and therefore in droplet viscosity) for ellipsoidal capsule production had also been reported for dripping extrusion techniques [24, 42].

Thus, the fact that capsule shape regularity and high polymer concentrations cannot be satisfied at the same time represents an important limitation of the centrifugal encapsulation technique for biomedical applications.

The formation of a protuberance in centrifugal capsule production when using highly viscous biopolymer solutions has recently been shown to be due to an insufficient relaxation time of the droplet during its flight in air, before impacting the gelation solution [23]. This has been quantified with the definition of a Deborah number De_{fall}, that compares the relaxation time to the fall time, as it will be defined in Section 2. The same study has shown that increasing the fall height above a certain limit induces (i) higher velocities of the falling droplet and hence a more

[1] Also called tip or tail in the literature.

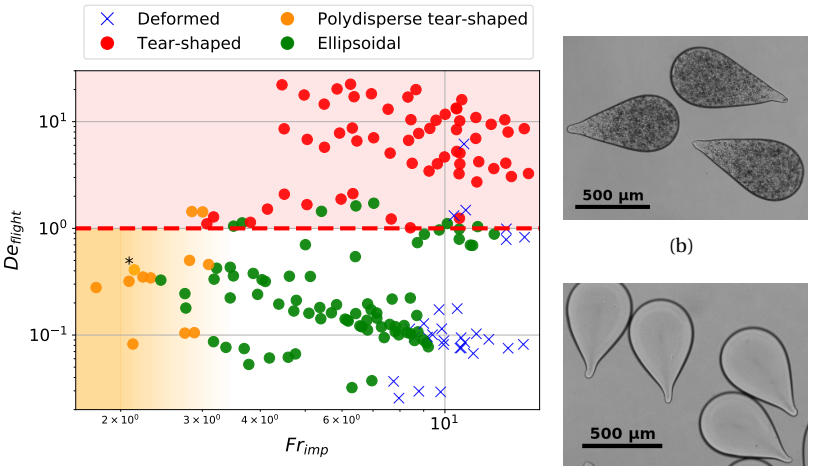

Figure 1. (a) Phase diagram from [23], showing the generation of capsules protuberance in the centrifugal encapsulation technique when using high viscosity alginate solutions, due to resulting Deborah numbers higher than unity. **(b) and (c)** Examples of tear-shaped capsules both with an encapsulated cargo (THP-1 cells, (b)) and without cargo (c).

violent impact on the surface of the gelation solution, damaging or breaking the droplet; (ii) a risk that the droplet impacts the container walls before reaching the gelation solution, due to its non-rectilinear trajectory in the centrifugal field. So, the flight time in air cannot be increased above a certain threshold. In this paper we put forward a technique allowing to go beyond this limitation. The design idea is based on the work of Buthe et al. [1] in the context of gravitational dripping encapsulation, who added several layers of immiscible liquid on top of the gelation bath, slowing down the alginate droplet and thus increasing the time available for shape relaxation, therefore helping to improve a spherical shape recovery before gelation. In that study the alginate solutions used were not highly viscous, so the question of tail formation (tear-shaped capsules) was not addressed. Moreover, the question of the biotolerability of the intermediate organic solvent layers was not addressed either.

This paper is structured as follows. In Section 2, an analytical model that is used to evaluate the feasibility of the concept of soft landing in centrifugal encapsulation is introduced. In Section 3 we present the centrifugal encapsulation device and carry out an experimental screening of possible materials that can be used for the soft landing layer, in order to select the three best-performing candidates. In Section 4 we analyse in detail, through an experimental parametric study, the behaviour of the system using each of the three candidates. Finally, in Section 5 we confirm, through the experimental results, the results obtained with the model introduced in Section 2.

2. Physical basis

2.1. *Formation of tear-shaped capsules with the standard device*

Figure 2(a) shows a schematic representation of a standard centrifugal encapsulation device, described in detail in previous work [3, 23, 43]. In this paragraph we discuss the initial device without the improvement by the soft landing layer. As mentioned in the introduction, the formation of

capsules with protuberance in standard centrifugal systems when using highly viscous polymer solutions has been shown in [23] to be due to a short relaxation time after extrusion and before gelation. Two time scales determine this behaviour:

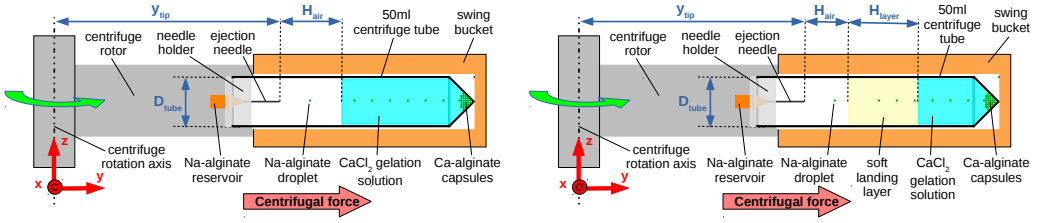

Figure 2. (a)-(b) Schematic representation of the centrifugal encapsulation device: (a) standard device without a soft landing layer (figure adapted from [23]); (b) improved device with a soft landing layer (figure adapted from [23]).

(1) the travel time of the droplet before its gelation, t_{fall}. In the standard device, this time is equal to the travel time in air t_{air}. This time can be estimated using a dynamic point mass model for the droplet motion between the ejection from the capillary and the entry in the gelation solution, as will be detailed below. In [23] it has been shown that for the droplet motion in air the drag term can be neglected in the equations of motion and a simple estimation of t_{fall} can be found:

$$t_{fall} = t_{air} = \frac{1}{\omega}\sqrt{\frac{2H_{air}}{y_{tip} + H_{air}/2}} \tag{1}$$

where ω is the angular velocity, y_{tip} the radial position of the capillary tip and H_{air} the distance between the capillary tip and the gelation bath.

(2) the characteristic relaxation time of the droplet, τ_{rel}. Based on a first modelling effort by Taylor [44], Luciani et al. developed an analytical description of the relaxation of an ellipsoidal drop toward a spherical shape under the assumption of relatively small deformations [45]:

$$\mathscr{D}(t) = \mathscr{D}_0 \exp\left(-\frac{80(m+1)}{(2m+3)(19m+16)}\frac{\gamma}{\eta_o D_{drop}}t\right) \tag{2}$$

where $\mathscr{D}$ is the dimensionless deformation of the ellipsoidal droplet defined using its major and minor axis A and B: $\mathscr{D} = (A-B)/(A+B)$; $\mathscr{D}_0$ is the deformation at $t = 0$; m is the ratio between the viscosity of the droplet fluid η_i and the viscosity of the surrounding fluid η_o; γ is the surface tension of the droplet fluid and D_{drop} is the equivalent diameter of a spherical droplet with the same volume. In the case of a liquid drop in air or of a very viscous drop inside a low-viscosity fluid ($m >> 1$), which is always the case in our system, equation (2) can be simplified as follows [46]:

$$\mathscr{D}(t) = \mathscr{D}_0 \exp\left(-\frac{40}{19}\frac{\gamma}{\eta_i D_{drop}}t\right) \tag{3}$$

We will use the characteristic decay time of this exponential function as an estimation of the characteristic relaxation time of the tail formed on alginate droplets in our system:

$$\tau_{rel} = \frac{19}{40}\frac{\eta_{alg} D_{drop}}{\gamma_{alg}} \tag{4}$$

where η_{alg} is the viscosity and γ_{alg} the surface tension of the alginate droplet.

These two time scales can be compared by the definition of a Deborah number:

$$De_{fall} = \frac{\tau_{rel}}{t_{fall}} \tag{5}$$

If $De_{fall} > 1$, the time available to a droplet before impacting the gelation bath is shorter than the time it needs to relax to a spherical shape. Thus, when the droplet begins to gel, a tail is still present and the gelation reaction will freeze it into a tear-shaped capsule. It has been shown that using the standard device (Figure 2(a)), in the case of medium to high concentrations of alginate, De_{fall} was always superior to unity, which causes the production of capsules with protuberance [23] (see Figure 1(a)).

Increasing t_{fall} can be done by increasing the fall height H_{air}, by decreasing the rotation velocity ω, or by changing the properties (typically viscosity and density) of the medium in which the droplet falls before entering the gelation solution. The first solution can only be used in a limited manner, since a too large fall height increases the risk both of a droplet impact with the tube wall and of damage or deformation of the droplets upon impact with the gelation bath, due to higher impact velocities. The second solution is also not convenient, because decreasing ω will modify the capsule size and decrease the droplet production frequency. In this paper, we propose using the third solution, which has been employed previously for capsule shape optimisation in dripping systems, called the "soft landing" approach [1, 47].

2.2. *Using a soft landing layer approach to increase droplet transit times t_{fall}*

The principle of soft landing is the following: we introduce a layer of an immiscible liquid on top of the gelation solution, as shown in Figure 2(b). The purpose of this liquid layer is to slow down the droplet long enough, so that it can relax to a spherical shape, before it reaches the gelation solution. If we denote t_{layer} the travel time of the droplet in the immiscible liquid layer, the total transit time t_{fall} of the droplet before reaching the gelation solution becomes:

$$t_{fall} = t_{air} + t_{layer} \tag{6}$$

Two properties of the immiscible liquid in the layer influence the transit of the polymer droplet through this layer: its density (which determines the buoyant force $\vec{F}_{Buoyancy}$) and its viscosity (which affects the hydrodynamic drag force $\vec{F}_{Drag}$ through the drag coefficient C_D), as shown in the set of equations (9). In the following we will refer to this liquid as the "soft-landing layer". We denote its thickness H_{layer}, the air gap between its surface and the ejection needle H_{air}, and define its relative thickness as:

$$h_{layer} = \frac{H_{layer}}{H_{air} + H_{layer}} \tag{7}$$

In this section we use an analytical model to study the feasibility of using a soft landing approach to increase the droplet relaxation time before gelation. In order to assess the travel time and trajectory of the droplet in the different fluids, we propose the following droplet motion model in the reference frame rotating with the centrifuge, based on [23]:

$$m_{drop}\frac{d\vec{v}}{dt} = \vec{F}_{Centrifugal} + \vec{F}_{Buoyancy} + \vec{F}_{Coriolis} + \vec{F}_{Drag} + \vec{F}_{Gravity} \tag{8}$$

with the following expressions of the forces:

$$\begin{aligned}
\vec{F}_{Centrifugal} &= -\rho_{alg} V_{drop} \vec{\omega} \times (\vec{\omega} \times \vec{r}) \\
\vec{F}_{Buoyancy} &= \rho_{fluid} V_{drop} \left[\vec{\omega} \times (\vec{\omega} \times \vec{r}) - \vec{g}_E\right] \\
\vec{F}_{Coriolis} &= -2\rho_{alg} V_{drop} \vec{\omega} \times \vec{v} \\
\vec{F}_{Drag} &= -\frac{1}{2} C_D \rho_{fluid} A_{drop} |\vec{v}| \vec{v} \\
\vec{F}_{Gravity} &= \rho_{alg} V_{drop} \vec{g}_E
\end{aligned} \tag{9}$$

Here, $\vec{\omega} = (0,0,\omega)$ is the rotation vector, aligned with the centrifuge rotation axis z and with constant rotating velocity ω; $\vec{r}$ is the position of the droplet, $\vec{v}$ the velocity of the droplet; ρ_{alg} and ρ_{fluid} the densities of alginate solution and surrounding fluid; C_D is the drag coefficient of the alginate droplet moving in the surrounding fluid, estimated for example using the correlation from Rivkind and Ryskin [48]; the droplet cross-section is $A_{drop} = \pi D_{drop}^2/4$; $\vec{g}_E = (0,0,-g_E)$ is the gravitational acceleration, with $g_E = 9.81\ m/s^2$.

The following initial conditions are assumed:

$$\begin{aligned}
\vec{r}(t=0) &= \vec{r}_{tip} = \left(x_{tip}, y_{tip}, 0\right) \\
\vec{v}(t=0) &= \vec{0}
\end{aligned} \tag{10}$$

The first condition indicates that the droplet is initially situated at the tip of the ejection needle. The reference system is chosen in such a way that the tip of the ejection needle is located in the $z = 0$ horizontal plane. The second condition assumes a zero initial velocity, given the quasistatic droplet formation. Compared to the case of droplet motion in air, in the case of droplet motion in the immiscible liquid of the soft landing layer the density ratio ρ_{alg}/ρ_{fluid} is orders of magnitude smaller. As a result, the drag force cannot be neglected in the calculation, and all the terms in equation (8) must be kept, hampering a simple analytical solution as the one of equation (1). Therefore a numerical solution is performed by integrating the ODE (8) numerically in time, in order to compute the trajectory and transit times of the droplet in the different media.

Let us now consider the following example: for a typical operating point where tear-shaped capsules are formed in the standard centrifugal encapsulation system, we perform a calculation of the transit time of the droplet before reaching the gelation solution, both with and without a soft landing layer. The parameters are listed in Table 1. For the soft landing layer in this example we will use soybean oil, which is immiscible with water, lighter than water and biocompatible; for the droplet we use a Na-alginate solution at 40g/L, i.e. 4% w/v.[2].

When using a soft landing layer, a first solution of equation (8) in air yields the droplet impact position on the surface of the soft landing layer. With the assumption that the droplet velocity falls to zero rapidly after the impact, a second solution of equation (8) is then performed inside the soft landing layer, using as initial conditions the impact position and a zero initial velocity.

Table 1 gives the computed transit times of the droplet in air t_{air} and in the liquid layer t_{layer}, as well as the characteristic relaxation time of the droplet τ_{rel}. It can be more convenient to define the relative transit times compared to the relaxation time: $t^*_{air} = t_{air}/\tau_{rel}$ and $t^*_{layer} = t_{layer}/\tau_{rel}$. Thus, the Deborah number is equal to:

$$De_{fall} = \frac{1}{t^*_{air} + t^*_{layer}} \tag{11}$$

The computed results show that by introducing only 20 mm of soft landing layer, the total transit time of the droplet before gelation increases of orders of magnitude, becoming higher than the

[2] Detailed properties in Section 3.1.

Table 1. Illustrative example for the feasibility of the soft landing approach in the centrifugal encapsulation system. c_{alg} is the concentration of the alginate solution in the droplet. D_{cap} is the inner diameter of the ejection capillary.

Case	c_{alg} (g/L)	D_{cap} (mm)	ω (RPM)	H_{air} (mm)	H_{layer} (mm)	t_{air} (ms)	t_{layer} (ms)	τ_{rel} (ms)	De_{fall}
No soft landing	40	0.20	2442	30	0	3.6	0	25.3	7.03
With soft landing	40	0.20	2442	10	20	1.96	508.2	25.3	0.05

relaxation time, resulting in a Deborah number lower than unity.[3] This example shows that the passage of the droplet through a soft landing layer could help extend the total droplet transit time so that the droplet tail has enough time to relax before entering into the gelation solution.

3. Experimental screening for materials

In order to address the problem of generating capsules without protuberance from highly viscous alginate droplets, we will proceed in two steps:

- Firstly, a number of candidate liquids are proposed for the soft landing layer. In this section, an experimental screening of these candidates is performed in order to retain the three liquids that produce the best and most robust results.
- In Section 4, a parametric study is carried out with the three selected liquids in order to find regions in the parameter space where spherical, or more in general ellipsoidal capsules are produced.

In the following paragraphs, we discuss the procedure used for the screening of candidate liquids for the soft landing layer and the results of this screening.

3.1. *A priori selection criteria for materials*

The candidate liquids for the soft landing layer must have certain properties in order to achieve the desired function: a density lower than that of the gelation bath (which is practically the same as water density), immiscibility with the aqueous gelation solution, so to form a mechanically stable layer on top of the gelation solution, and biotolerability (for biomedical encapsulation applications). In this study, seven candidates have been chosen for investigation, which can also be regarded as representatives of different groups of liquids (vegetable oils, mineral oils, synthetic oils, deep eutectic liquids, solvents). The properties of these liquids are listed in Table 2. To produce the alginate droplets we use a Na-alginate solution at 40g/L (see Table 2 for properties). No surfactant is used in the experiments in this work, due to the potential inhibitory effects on the encapsulated material in biomedical applications [49].

The choice of the different vegetable oils is obvious, since they are known to be biotolerable. The biotolerability of DLMA has been studied in [52]. While most of the solvents, like the ones used by Buthe et al. [1] are not biotolerable, one study has shown that short exposure (under a few minutes) of cells to n-Decane does not reduce cell viability [54]. That is why n-Decane was also chosen as a candidate for the soft landing layer.

[3] Other computations of total transit times depending on the properties of the soft landing layer are given in the supporting information S.3.

Table 2. Properties of the liquids used as candidates for the soft landing layer and of the alginate solution.

Category	Liquid	Density (g/cm^3)	Viscosity ($mPa.s$)	Surface tension (mN/m)
Synthetic oil	PDMS[g]	0.913[a]	5.0[a]	26.4[b]
Deep eutectic liquid	DLMA[h]	0.90[e]	33.2[e]	n.a.
Solvent	n-Decane[i]	0.73[a]	0.85[a]	23.0[b]
Vegetable oil	Almond oil[j]	0.91[a]	71[c]	n.a.
Vegetable oil	Soybean oil[k]	0.92[a]	60[a]	20.7[b]
Vegetable oil	Corn oil[l]	0.92[a]	68[f]	n.a.
Mineral oil	Parffin oil[m]	0.83...0.89[a]	110...230[a]	n.a.
Na-Alginate	Alginate[n] 40g/L	1.02[p]	$15.2 \cdot 10^3$ [p]	72[p]

[a] Average reference values from manufacturer. [b] Surface tension in water, measured using the pendant droplet method (Krüss DSA100, Germany). [c] Values taken from the literature [50]. [d] Values taken from the literature [51]. [e] Values taken from the literature [52]. [f] Values taken from the literature [53]. [g] Sigma 317667 (Sigma-Aldrich, USA). [h] DL-Menthol: Sigma W266507 (Sigma-Aldrich, USA) and Lauric Acid: Sigma W261408 (Sigma-Aldrich, USA). [i] Sigma 8.03405 (Sigma-Aldrich, USA). [j] Sigma 63445 (Sigma-Aldrich, USA). [k] Roth 3686 (Carl Roth, Germany). [l] Acros 405435000 (Thermo Fisher Scientific, USA). [m] Sigma 18512 (Sigma-Aldrich, USA). [n] PRONOVA SLG100 (Novamatrix, Norway). [p] Values from [3,23].

3.2. *Control parameters for the screening experiments*

A series of capsule generation experiments was performed with each of these liquids in order to identify the most suitable candidates. For each candidate liquid, three experiments were carried out with different rotation velocities. The rotation velocity was varied because it is one of the main parameters controlling the transit time of the droplet in air and in the soft landing layer, as well as the velocity of the droplet during the transit. The inner diameter of the ejection capillary was adapted for high rotation velocities in order to avoid ejection in a jetting regime. The control parameters for these experiments are listed in Table 3.

3.3. *Results of the screening experiments*

Qualitative results from the screening experiments are presented in Figure 3. For each of the three experiments and for each of the liquids tested, we show a representative image of capsules that were generated. The main criteria for the selection of a candidate are the ability to produce capsules without protuberance, the regularity of capsule shapes (ellipsoidal), and the monodispersity of the capsule sizes.

The vegetable oils (almond, corn and soybean) have a roughly similar performance, due to their similar properties. For low rotation velocities, all of them generate some capsules with protuberance. For middle and high rotation velocities, both the almond oil and the soybean oil experiments show the production of capsules which are more uniform in shape and roughly

Table 3. Parameters used in the screening experiments.

	H_{air} (mm)	H_{layer} (mm)	D_{cap} (mm)	c_{alg} (g/L)	ω (RPM)	$[CaCl_2]$ (mM)
Experiment 1	15	28	0.410	40	1221	100
Experiment 2	15	28	0.410	40	1865	100
Experiment 3	15	28	0.200	40	2442	100

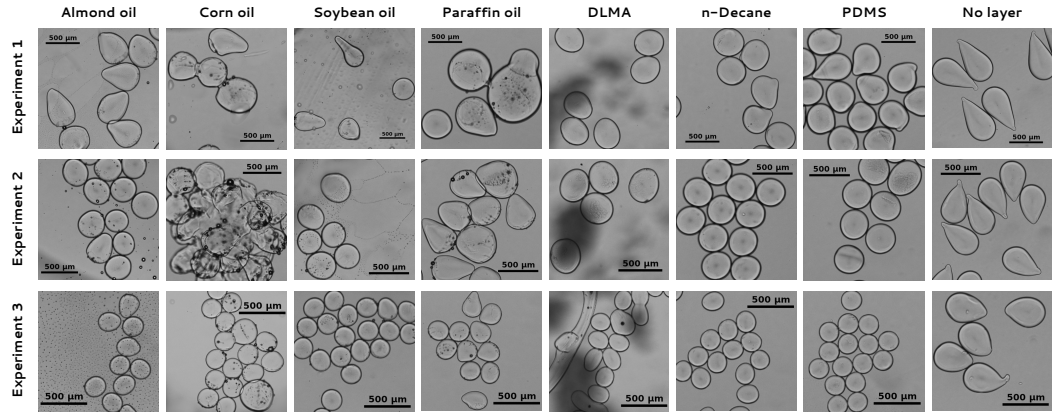

Figure 3. Results of the screening experiment with each of the seven candidate liquids, for the three experiments. The column labelled "No layer" at the right shows results of experiments without the soft landing layer ($H_{layer} = 0$), keeping all other parameters constant.

monodisperse in size. The corn oil, however, generates an aggregate of capsules for middle velocities and polydisperse-sized capsules for higher velocities. Between the almond oil and the soybean oil, the latter was retained as a candidate for the immiscible liquid layer, due to the slightly better performance and the significantly lower cost.

The experiments with paraffin oil generated polydisperse and tear-shaped capsules in all three cases, which justifies its rejection as a potential candidate.

The experiments with the deep eutectic liquid DLMA produced fairly uniformly shaped capsules for low and medium rotation velocities. However, at high rotation velocities, the capsules were not regular in shape and size, and the formation of long fibres was also observed, for which a clear explanation is not yet available. Moreover, the DLMA seems to react with the salts in the gelation solution and produce white aggregates at the interface with the gelation solution (giving the shaded regions in the corresponding images in Figure 3), that eventually fragment and sink to the bottom. These could represent a hindrance for the formation of capsules, therefore the DLMA was not further considered as a candidate for the soft landing technique.

Finally, remarkably good results were obtained with both n-Decane and PDMS as soft landing layer. For lower rotation velocities, the presence of a protuberance on some capsules was still observed, but for middle and higher rotation velocities both the liquids produce capsules with regular shapes and relatively uniform sizes. Therefore, both these liquids were retained, along with the soybean oil, as candidates for the soft landing layer in the centrifugal soft landing technique. The use and performances of these three liquids as soft landing layer will be analysed experimentally in Section 4.

4. Experimental study of the three selected materials

Once two or three candidates for the immiscible liquid layer were identified after the screening experiments, a parametric study was carried out with the selected liquids, in order to identify regions of optimal operation of the centrifugal encapsulation device with the immiscible liquid layer, using highly viscous alginate solutions. The main two parameters that were varied are the rotation velocity and the depth of the soft landing layer, since they both control the transit times and velocities of the droplets in the soft landing layer:

- For the rotation velocity, four values were chosen corresponding to a medium-to-high range for this device. This range is relevant for applications, since a higher rotation velocity increases the production frequency of the capsules.
- Four different depths of the soft landing layer were tested, from a relatively small value (less than half of the fall height in air) to a relatively large value (four times the fall height in air). A soft landing layer with a thickness lower than 5 mm would not increase significantly the transit time of the droplet and might be more sensitive to the effect of its two bordering interfaces. A thickness much higher than 40 mm is not reasonable in our device for two reasons: (i) enough gelation bath should be left below for an efficient gelation of the droplet and avoiding aggregate formation on the bottom of the tube [23]; (ii) the droplet trajectory is not parallel to the tube axis and the droplet might reach the tube wall during transit in the soft landing layer, which might generate an undesired behaviour and deformation of the droplet.

The diameter of the ejection capillary was chosen adequately for each centrifugation speed in order to avoid an ejection in jetting regimes [23]. The alginate concentration was kept constant and the value was chosen in the region where tear-shaped capsules were obtained with the standard device. The viscosity of the alginate solution at this concentration is around 15 $Pa.s$ [3]. The fall height in air H_{air} was kept constant, so that an increase of H_{layer} corresponds to a decrease of the depth of the gelation solution, for two reasons: (i) its effect on droplet relaxation is much less significant than that of the soft landing layer thickness (see Table 6); (ii) a large fall height in air leads to a high impact velocity with the air-liquid interface, that can possibly damage or deform the droplet and hamper comparison between the experiments.

A summary of the operating points explored in the parametric study is listed in Table 4.

4.1. *Overview of possible capsule shapes*

Before analysing in detail the results of the parametric study for each of the three liquids, let us first give an overview of the different types of capsules that could be obtained. Figure 4 shows examples of capsules shapes and some combinations of these features. Figures 4(a) and 4(b) show spherical and ellipsoidal capsules. Such protuberance-free uniformly shaped monodisperse capsules could be obtained with all three candidate liquids with certain combinations of parameters, as we will show later. These results are a confirmation of the successful use of the soft landing method for the generation of ellipsoidal capsules from highly viscous alginates in centrifugal encapsulation devices.

Figure 4(c) shows an experiment where capsules were highly polydisperse in size. The large capsules are most probably a result of a coalescence of alginate droplets. Since in the standard centrifugal encapsulation device droplet coalescence is extremely rarely observed [3, 23], the coalescence most likely takes place inside the soft landing layer, before entering the gelation

Table 4. Parameters varied in the parametric study. SO stands for soybean oil and nD for n-decane.

	Series 1	Series 2	Series 3	Series 4
Liquid	nD, SO, PDMS	nD, SO, PDMS	nD, SO, PDMS	nD, SO, PDMS
H_{layer} (mm)	5, 19, 33, 40	5, 19, 33, 40	5, 19, 33, 40	5, 19, 33, 40
D_{cap} (mm)	0.410	0.200	0.200	0.100
c_{alg} (g/L)	40	40	40	40
H_{air} (mm)	10	10	10	10
ω (RPM)	1865	2115	2442	3153

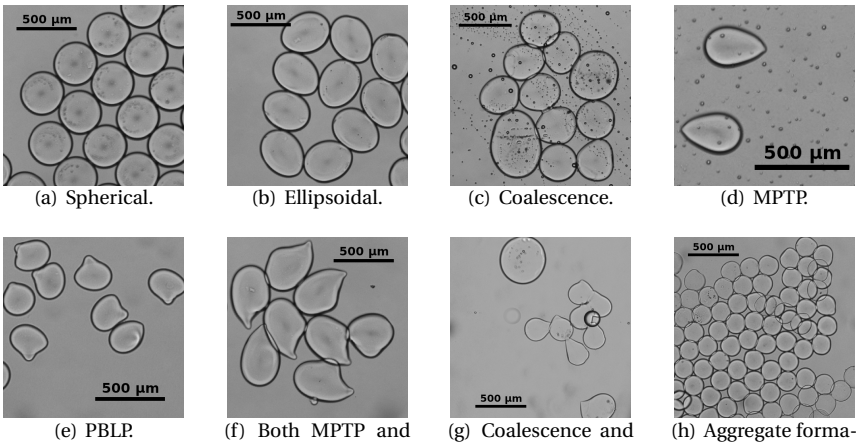

(a) Spherical. (b) Ellipsoidal. (c) Coalescence. (d) MPTP.

(e) PBLP. (f) Both MPTP and PBLP. (g) Coalescence and PBLP. (h) Aggregate formation.

Figure 4. Examples of capsules obtained in the parameteric study.

solution. One can suppose that two successive droplets may come into contact due to the very low sedimentation velocity in the soft landing layer, given by a low density ratio.

Figure 4(d) shows an example of tear-shaped capsules, that present the following features: (i) they are monodisperse in size and shape; (ii) they feature a pointed "tip" on the protuberance which seems to be a remainder of the broken ligament which was connecting the drop to the rest of the alginate in the capillary at the moment of detachment; (iii) this tip is aligned with the longitudinal axis of the capsule. These features indicate a protuberance formation mechanism by insufficient relaxation of the droplet before gelation, as discussed in detail in [23]. When this type of capsules is obtained, it indicates that the slowing down of the droplets in the soft landing layer was not long enough to allow a full relaxation of the droplet to a spherical shape. In this paper, we will use the term monodisperse pointed-tip protuberance (MPTP) for capsules featuring these characteristics.

Figure 4(e) shows examples of polydisperse tear-shaped capsules, which are different from the tear-shaped capsules introduced above by the following features: (i) the protuberances are polydisperse in size and shape; (ii) some circular lines are present at the basis of the protuberance; (iii) the protuberance is often rounded at the tip (it has the aspect of a bump) and does not feature a pointed tip that could be identified as a remnant of a broken ligament; (iv) if the capsule body has an ellipsoidal shape, the protuberance is often not aligned with the longitudinal axis of the capsule body. These characteristics are distinctive for another mechanism of protuberance formation, namely the attachment of the droplet to the interface between the two fluids during gelation [23]. In the case of an interface between air and gelation solution, this phenomenon occurs very rarely, when droplets impact the solution with very low velocities [3, 55]. However, in the case of an interface between the gelation solution and an overlying immiscible liquid, this phenomenon has been reported in multiple studies in the literature [38, 56–59]. These studies showed that this phenomenon is very limiting for ellipsoidal capsule production, and requires special treatments with pre-gelation steps when gravity with no centrifugation is used to sediment the droplets. Regarding the nomenclature that will be used to describe this kind of shapes, while characteristic (i) is universal for this type of protuberance and is present in all the cited studies, the other characteristics (ii-iv) have been noticed mostly in centrifugation experiments with and without a soft landing layer ([3] and the present study). This is why for capsules featuring these shape characteristics the term "polydisperse bump-like protuberance" (PBLP) will be

used here specifically, whereas the term polydisperse protuberance would be more largely applicable to all the similar cases in the literature.

Additionally, Figures 4(f) and 4(g) show combinations of the three latter cases above. The capsules in Figure 4(f) present two protuberances: the first protuberance is aligned with the capsule longitudinal axis and has a pointed tip; the second protuberance is located laterally from the capsule longitudinal axis, and it has the aspect of a bump, rounded and with no pointed tip. Given the distinctive characteristics of the two protuberance formation mechanisms mentioned above, we believe that the two protuberances observed on this type of capsules correspond to the coexistence of the two different mechanisms. Moreover, the location of the protuberance which we attribute to the attachment to the interface during gelation, located on the side of the prolate tear-shaped capsules, might indicate the orientation the droplets had while crossing the interface between the two liquids and started gelling [23].

Finally, in some experiments the formation of aggregates of capsules on the bottom of the centrifuge tube was noticed (Figure 4(h)). This is different from coalescence, because these aggregates are most likely formed when a partially gelled capsule sediments on the bottom of the tube and sticks to the capsules which sedimented there before [23]. Depending on the application, the formation of aggregates may not be a major limitation since it does not alter the capsule shapes or monodispersity and it can usually be remedied relatively easily, just by agitating the solution. Due to these considerations, the formation of capsule aggregates on the tube bottom will not be further discussed in this paper.

A qualitative analysis of the capsule shapes, based on the criteria presented in this section, was carried out for each experiment in order to identify the types of capsule shapes obtained in that experiment. This is presented in the paragraphs below and will be used to assess the results of the microcapsule production experiments with a soft landing layer.

4.2. *Soybean oil*

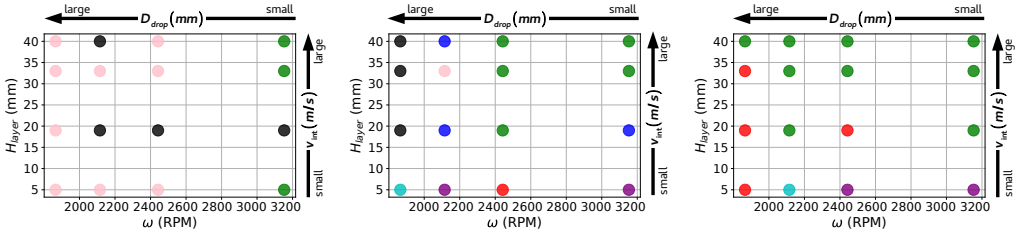

(a) Soybean oil. (b) PDMS. (c) n-Decane.

Figure 5. Results of the parametric study for each of the three liquids used as soft landing layer. **Green**: ellipsoidal capsules; **black**: coalescence, capsules without protuberance; **brown**: coalescence, capsules with MPTP; **pink**: coalescence, capsules with a PBLP; **cyan**: coalescence, capsules with both MPTP and PBLP; **red**: capsules with MPTP; **blue**: capsules with with PBLP; **purple**: capsules with both MPTP and PBLP.

Results of the parametric study using soybean oil as soft landing layer are shown in Figure 5(a). With soybean oil, coalescence was observed in many of the experimental points, especially at a low thickness of the liquid layer and low rotating velocities. These are linked in our experiments with larger droplet diameters D_{drop} and lower velocities at the interface v_{int}. Without the ability to visualise the droplet trajectory in the liquids during the centrifugation, it is not simple to predict

where and why this coalescence of the drops takes place. The fact that coalescence takes place at lower rotating velocities, might correlate with a slower crossing of the soft landing layer and of the interface of the interface of the gelation solution, resulting in a higher probability of successive droplets to meet inside the soft landing layer.

For soybean oil, the formation of a protuberance by insufficient relaxation (MPTP) was not observed. This probably due to the higher viscosity of the soybean oil compared to the other liquids, which increases the transit time of the droplet in the soft landing layer, giving it sufficient time to relax to a spherical shape (cf. Table 6).

On the other hand, the formation of capsules with a PBLP, linked to an attachment to the interface between the two liquids, was observed in many of the experiments with using soybean oil as soft landing layer, coupled with the coalescence and especially for low rotation velocities. Lower rotation speeds, as well as larger droplet diameters, lead to a lower velocity of the droplet. The study in [23] showed that the ability of a droplet to cross an interface correlates with the Froude number at the interface $Fr_{int} = v_{int}/\sqrt{g_{int}D_{drop}}$, where v_{int} is the velocity of the droplet before reaching the interface, g_{int} is the centrifugal acceleration at the location of the interface and D_{drop} the diameter of the droplet. A low Froude number, implying low velocities of the droplet at the interface and/or large droplet diameters, favours the attachment to the interface and the formation of a PBLP. This is confirmed in the experiments with soybean oil, where protuberance-free capsules were obtained only for smaller droplet diameters and larger velocities at the interface.

Globally, using soybean oil as soft landing layer provided good results mostly for small droplet diameters, larger depths of the soft landing layer and for large velocities of the droplet at the interface.

4.3. *PDMS*

The results of the parametric study for the PDMS soft landing layer are plotted in Figure 5(b). Firstly, less cases of coalescence were observed compared to the soybean oil, and these are all found for the lowest rotating velocity (and highest droplet diameter). As discussed in the previous section, this is probably related to a slower crossing of the soft landing layer and of the interface and thus a larger probability of successive droplets meeting inside the soft landing layer.

Secondly, insufficient relaxation occurs more often in the case of PDMS, although only for the smallest height of the soft landing layer. Since PDMS has a similar density but significantly lower viscosity than soybean oil, the droplet transit times in the soft landing layer are shorter (see Table 6), which explains why more cases of insufficient relaxation were observed.

At the same time, more cases of PBLP formation were obtained using PDMS as soft landing layer. Similarly to the experiments with soybean oil, this phenomenon is correlated with the Froude number at the interface. For smaller droplet diameters and higher velocities at the interface, implying a larger Froude number at the interface, capsules without protuberance could be produced.

Although the parametric study using PDMS yielded slightly more successful results than using soybean oil, the same tendency has been noticed: in general monodisperse ellipsoidal capsules are obtained for smaller droplet diameters and large depths of the soft landing layer, inducing larger velocities at the interface between the soft landing layer and the gelation solution.

4.4. *n-Decane*

Using n-Decane as soft landing layer has yielded globally the most satisfactory results.

Coalescence was observed in only one of the experimental points, for a low thickness of the n-Decane layer and low rotating velocity (large droplet diameter), implying a low Froude number at the interface.

On the other hand, the formation of capsules with MPTP occurred more frequently when using n-Decane, compared to the other two liquids. The lower viscosity and density of the n-Decane cause a faster transit of the droplet through the soft landing layer (see Table 6). Especially for small heights of the liquid layer, this transit time is not long enough to allow the droplet shape to relax before reaching the gelation solution (De_{fall} numbers are higher than unity). This leads to the formation of capsules with MPTP for these cases.[4]

The formation of PBLP was observed in the experiments with low thickness of the soft landing layer, which is correlated with a lower velocity at the interface. Secondly, the small values of H_{layer} induce a higher uncertainty in the calculation of the droplet motion inside the soft landing layer, because side effects and interface effects may become more important. This might lead to an overestimation of the velocity at the interface in this case.

The experiments with n-Decane yielded the largest number of successful results in the explored parametric region and seem to be the most predictable and controllable: using a soft landing layer with sufficient depth, n-Decane can be successfully employed to form monodisperse ellipsoidal capsules from very viscous alginate solutions.

4.5. *Summary of the results*

Table 5. Summary of the results of the parametric study: number of experiments in the parametric study (out of all experiments carried out with the respective candidate liquid) where an undesirable characteristic was observed.

Liquid	Coalescence	MPTP	PBLP	Ellipsoidal monodisperse	Total
Soybean oil	13 **(81%)**	0 **(0%)**	9 **(56%)**	3 **(19%)**	16 **(100%)**
PDMS	5 **(31%)**	4 **(25%)**	7 **(44%)**	5 **(31%)**	16 **(100%)**
n-Decane	1 **(6%)**	7 **(43%)**	3 **(19%)**	9 **(56%)**	16 **(100%)**

The results of the parametric study with the three different liquids are summarised in Table 5. It can be seen that ellipsoidal monodisperse capsules could be obtained with all the three candidate liquids, in various configurations. Coalescence of droplets seems more likely to occur for the more viscous and denser liquids, whereas the formation of MPTP is more likely for the less viscous and less dense fluids. Regarding the occurrence of PBLB formation, the results indicated that it is lower when using large rotating velocities and large depths of the soft landing layer.

5. Modelling of the three selected materials

5.1. *Transit times and the Deborah number*

The theoretical model presented in Section 2 was used to calculate the transit times of the droplets in air and the soft landing layer for each of the experiments performed in the parametric

[4]The experiments with $H_{layer} = 19\ mm$ reported in Figure 5(c) are located very close to the transition limit between ellipsoidal capsules and MPTP formation. The experimental uncertainty causes some of these experiments to fall in the ellipsoidal regime and others in the MPTP formation regime, which gives the impression of a non-monotonic evolution of the resulted shape with the control parameters (alternating green and red points). Examples and more discussion is given in the supporting information S.4.

Table 6. Computed droplet transit times for the three candidate liquids in the four experimental series. The bold values indicate experiments where capsules with MPTP were formed.

	τ_{rel} (ms)	t^*_{air}	**Soybean oil**				**PDMS**				**n-Decane**			
H_{layer} (mm)			5	19	33	40	5	19	33	40	5	19	33	40
Series			t^*_{layer}				t^*_{layer}				t^*_{layer}			
1	39.7	0.06	2.6	9.32	15.3	18.1	**0.47**	1.66	2.76	3.27	**0.14**	**0.48**	**0.79**	0.94
2	28.7	0.08	5.18	18.6	30.6	36.1	**0.76**	2.73	4.54	5.38	**0.21**	0.71	1.18	1.4
3	26.1	0.08	5.19	18.6	30.6	36.1	**0.76**	2.72	4.52	5.37	**0.20**	**0.70**	1.17	1.39
4	17.5	0.09	10.2	36.5	60.1	70.9	**1.3**	4.6	7.6	9.01	**0.3**	1.06	1.76	2.09

study with the three candidate liquids[5]. The relative transit times t^*_{air} and t^*_{layer}, as well as the characteristic relaxation time τ_{rel}, are reported in Table 6. The bold values in the table represent experiments where capsules with MPTP were observed. These results show that the formation of MPTP correlates with the condition $t^*_{air} + t^*_{layer} < 1$, which describes an insufficient time for droplet relaxation.

In order to better visualise these results, Deborah numbers for the droplets in each of the experimental points are computed using equation (11). In Figure 6 we plot the De_{fall} number and the relative thickness of the soft landing layer of liquid h_{layer} for each experimental point. Red crosses were used to mark the experiments where tear-shaped capsules were produced, i.e. where the distinctive features of a protuberance attributed to insufficient relaxation of the droplet are noticed, according to the criteria discussed in the previous section. These also include the experiments where capsules with two protuberances were formed. All other experiments, where such protuberances could not be identified, were marked with green circles. In some cases, the De_{fall} and h_{layer} numbers of two experiments are very close to each other, which leads to the superposition of the markers on the plot, as it is the case for two experiments with $De_{fall} \approx 1.5$ and $h_{layer} \approx 0.66$, giving different results. These two points correspond to experiments in the parametric study with n-Decane, with $H_{layer} = 19\ mm$ and $w = 2115\ RPM$ and $w = 2442\ RPM$ respectively. The produced capsules in both cases are very close to the limit between ellipsoidal capsules and MPTP capsules, as detailed in the supporting information S.4.

It can be noticed in Figure 6 that the limit for protuberance formation due to insufficient droplet relaxation seems to be located around $De_{fall} = 1$, which was also previously shown for the standard centrifugal device without a soft landing layer [23]. This confirms that the model introduced in Section 2 can predict relatively well the transit times of the droplet in air and in the soft landing layer. For a low thickness of the soft landing layer, side effects and the hypothesis of zero initial velocity in the soft landing layer might introduce more uncertainty in this calculation, which might explain the results with $h_{layer} \approx 0.33$, where the transition to capsules with MPTP seems to occur at $De_{fall} \approx 0.7$.

5.2. *Contributions of different forces in slowing down the droplet*

At this point, one may wonder which characteristic of the soft landing fluid is dominant in slowing down the droplets. Indeed, both density and viscosity can play a role, the former through a modification of buoyancy, the latter through a modification of drag.

In order to investigate more in detail the contribution of the different forces in slowing down the droplet inside the soft landing layer, we can use the droplet motion model introduced in

[5]Other results from the computations, such as droplet trajectories or forces acting on the droplet, are given in the supporting information S.1 and S.2.

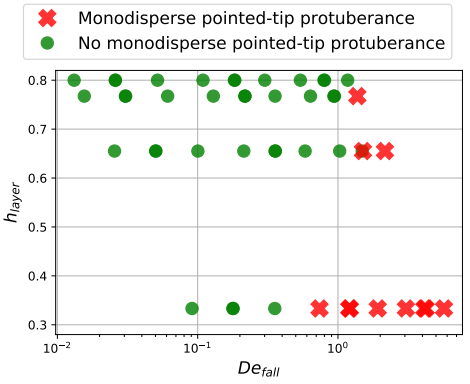

Figure 6. Formation of capsules with a protuberance due to insufficient relaxation as a function of the Deborah number and the height of the soft landing layer.

Section 2 to calculate the mechanical work of each of the forces involved (set of equations (9)), according to the following definition:

$$W_F = \int_{t_0}^{t_1} \vec{F} \cdot \vec{v} \, dt \tag{12}$$

where $t_1 - t_0$ is the theoretical transit time of the droplet inside the soft landing layer. The theorem of kinetic energy states that the total work[6] done on a particle during a time lap is equal to the variation of its kinetic energy E_k [60]:

$$W_{Centrifugal} + W_{Buoyancy} + W_{Drag} + W_{Gravity} = \Delta E_k \tag{13}$$

Normalising the different terms by the work of the centrifugal force, we obtain the equation:

$$\Delta E_k^* - W_{Buoyancy}^* - W_{Drag}^* - W_{Gravity}^* = 1 \tag{14}$$

where the star superscript indicate values normalised by $W_{Centrifugal}$.

Table 7. Computed mechanical work of the forces involved in the droplet motion, normalised by $W_{Centrifugal}$, which is practically equal for all soft landing fluids.

	ΔE_k^*	$W_{Buoyancy}^*$	W_{Drag}^*	$W_{Gravity}^*$	Re
Soybean oil	$6.86 \cdot 10^{-6}$	-0.902	-0.098	$2.1 \cdot 10^{-6}$	0.16
PDMS	$0.323 \cdot 10^{-3}$	-0.895	-0.105	$2.18 \cdot 10^{-6}$	13.1
n-Decane	$5.12 \cdot 10^{-3}$	-0.716	-0.279	$2.29 \cdot 10^{-6}$	245
Dense Air	$2.18 \cdot 10^{-3}$	-0.902	-0.096	$2.91 \cdot 10^{-6}$	9430
Viscous Air	$0.781 \cdot 10^{-3}$	$-1.18 \cdot 10^{-3}$	-0.998	$2.1 \cdot 10^{-6}$	$2.23 \cdot 10^{-3}$
Air	0.917	$-1.18 \cdot 10^{-3}$	-0.082	$3.15 \cdot 10^{-6}$	306

For each of the candidate liquids considered, the variation of the computed normalised work showed very little variation (usually lower than 1 %) between the four experimental series and the four depths of the soft landing layer. In Table 7, we present the results for one of the experimental points[7], which are representative of all the other experimental points for each liquid. Theoretical results with two hypothetical fluids as soft landing layer are given for comparison: “Dense Air” is

[6] The Coriolis force produces a null mechanical work by its definition, being perpendicular to the velocity vector.
[7] The chosen case was experiment series 3 with a soft landing layer depth of 19 mm.

a fluid with the properties of air but the density of soybean oil; "Viscous Air" is a fluid with the properties of air but the viscosity of soybean oil. The results in air (without soft landing layer) at equivalent fall height are also given. The computed Reynolds numbers $Re = \rho_{fluid} v D_{drop} / \eta_{fluid}$ at final velocity are also given for reference.

For the three real liquids tested, the buoyant force plays the dominant role in slowing down the droplet, while the rest is accomplished by the drag force. When comparing with the case in air, we see that the introduction of either a higher density or a higher viscosity is sufficient to significantly slow down the droplet (which can be seen in the final droplet kinetic energy). A combination of the two might help reduce the transit time, for achieving a full relaxation of the droplet to a spherical shape before gelation, and at the same time control the flow properties (Re number), for the optimisation of the system operation.

6. Conclusion and perspectives

In this paper we report for the first time the successful usage of a soft landing approach in a centrifugal microencapsulation device to generate monodisperse ellipsoidal capsules using high viscosity alginate solutions. This method is generic and applicable to different types of centrifugal encapsulation devices, including recent designs like in [18].

First, an analytical droplet motion model was used to highlight and quantify the phenomenon of insufficient relaxation of the droplets, which is the cause for the formation of capsules with protuberance when high viscosity alginates are used for encapsulation. The model confirmed the feasibility of using a soft landing approach to counter this phenomenon.

Then, a first series of experiments was carried out in order to find the best candidate liquids for the soft landing layer. Out of seven different candidates featuring three vegetable oils, one synthetic oil, one mineral oil, one solvent and one deep eutectic liquid, three candidates were selected based on their performance for producing monodisperse ellipsoidal capsules: soybean oil, PDMS and n-Decane. Secondly, a parametric study of microgel production was carried out with each of these liquids by varying the rotation velocity and the height of the soft landing layer, which both control the transit time inside the soft landing layer.

Successful monodisperse ellipsoidal capsules production was reported with all three candidate liquids, in operating points where tear-shaped capsules are produced with the standard centrifugal device (Figure 7). The best results were obtained for high rotating velocities, low droplet sizes and large depths of the soft landing layer, giving larger droplet velocities at the interface.

Three major limitations for the production of monodisperse ellipsoidal capsules with the soft-landing layer technique were identified. Firstly, as one would expect, experimental results show that the use of a too thin soft landing layer does not allow to obtain ellipsoidal particles and a thick enough soft landing layer must be used. This has been quantified with the introduction of a relevant Deborah number De_{fall} comparing relaxation time and fall time: the condition $De_{fall} < 1$ must be satisfied in order to ensure sufficient droplet relaxation before gelation. Secondly, coalescence of droplets occurred for large droplet diameters and low rotation speeds, mostly for the more viscous liquids, soybean oil and PDMS. This has been interpreted as being related to contact between drops within the soft landing layer. Thirdly, the formation of capsules with polydisperse bump-like protuberance was observed, for each of the tested liquids, at low velocities at the interface and large droplet diameters, which correlate with low interface Froude numbers Fr_{int}. This has been explained as being an effect of a slow interface crossing between the soft landing layer and the gelation solution.

The parametric study carried out in this work showed that the soft landing layer technique applied to centrifugal microencapsulation can work successfully with various liquids. For all the three candidate liquids examined here (soybean oil, PDMS and n-Decane), operating points

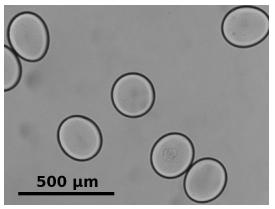

(a) n-Decane, $\omega = 2442\ RPM$, $H_{layer} = 33mm$, $H_{air} = 10mm$.

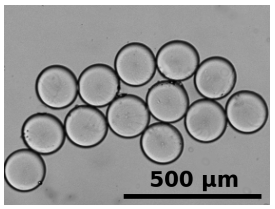

(b) Soybean oil, $\omega = 3153\ RPM$, $H_{layer} = 40mm$, $H_{air} = 10mm$.

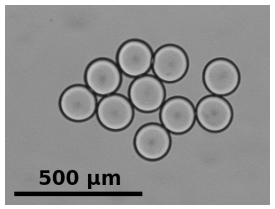

(c) PDMS, $\omega = 3153\ RPM$, $H_{layer} = 40mm$, $H_{air} = 10mm$.

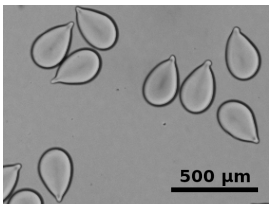

(d) No soft landing layer, $\omega = 2442\ RPM$, $H_{air} = 10mm$.

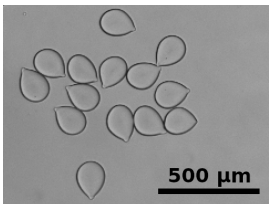

(e) No soft landing layer, $\omega = 3153\ RPM$, $H_{air} = 10mm$.

Figure 7. (a), **(b)** and **(c)**: Examples of successful ellipsoidal monodisperse capsule production with each of the three candidate liquids. **(d)** and **(e)**: Equivalent experiments without soft landing layer, showing the formation of capsules with protuberance.

could be found for successful ellipsoidal or spherical capsule production from highly viscous alginate solutions.

As future work, in order to move towards the biomedical applications, validation experiments could be carried out by encapsulating cells using the soft landing approach and measuring the viability and functionality of these cells compared to those encapsulated using the standard centrifugal encapsulation process. For the improvement of the device, in order to avoid coalescence in the soft landing layer when using soybean oil or PDMS, the usage of biocompatible surfactants could be tested. Another improvement could be to find alternative liquids with similar physical properties as the n-Decane, but with higher biotolerability. Finally, further work could be performed to give a finer description of the physical phenomena at play in the slowing down of the droplet inside the soft landing layer.

Conflicts of interest

The authors declare no competing financial interest.

References

[1] A. Buthe, W. Hartmeier, M. B. Ansorge-Schumacher, "Novel solvent-based method for preparation of alginate beads with improved roundness and predictable size", *J. Microencapsul.* **21** (2004), no. 8, p. 865-876.

[2] S. Haeberle, L. Naegele, R. Burger, F. Von Stetten, R. Zengerle, J. Ducree, "Alginate bead fabrication and encapsulation of living cells under centrifugally induced artificial gravity conditions", *J. Microencapsul.* **25** (2008), no. 4, p. 267-274.

[3] M. Badalan, F. Bottausci, G. Ghigliotti, J.-L. Achard, G. Balarac, "Three-dimensional phase diagram for the centrifugal calcium-alginate microcapsules production technology", *Colloids Surf. A Physicochem. Eng. Asp.* **635** (2022), article no. 127907.

[4] K. Maeda, M. Takinoue, H. Onoe, S. Takeuchi, "A centrifuge-based droplet shooting device for the synthesis of multi-compartmental microspheres under ultra-high gravity", in *15th International Conference on Miniaturized Systems for Chemistry and Life Sciences 2011, MicroTAS 2011*, vol. 1, 2011, p. 12-14.

[5] K. Maeda, H. Onoe, M. Takinoue, S. Takeuchi, "Controlled synthesis of 3D multi-compartmental particles with centrifuge-based microdroplet formation from a multi-barrelled capillary", *Advanced Materials* **24** (2012), no. 10, p. 1340-1346.

[6] K. Inamori, H. Onoe, M. Takinoue, S. Takeuchi, "Centrifuge-based single cell encapsulation in hydrogel microbeads from ultra low volume of samples", in *17th International Conference on Miniaturized Systems for Chemistry and Life Sciences, MicroTAS 2013*, vol. 1, Chemical and Biological Microsystems Society, 2013, p. 314-316.

[7] M. Hayakawa, H. Onoe, K. H. Nagai, M. Takinoue, "Rapid formation of anisotropic non-spherical hydrogel microparticles with complex structures using a tabletop centrifuge-based microfluidic device", in *17th International Conference on Miniaturized Systems for Chemistry and Life Sciences, MicroTAS 2013*, vol. 1, Chemical and Biological Microsystems Society, 2013, p. 630-632.

[8] H. Onoe, K. Inamori, M. Takinoue, S. Takeuchi, "Centrifuge-based cell encapsulation in hydrogel microbeads using sub-microliter sample solution", *RSC Adv.* **4** (2014), no. 58, p. 30480-30484.

[9] H. Yamashita, M. Morita, H. Sugiura, K. Fujiwara, H. Onoe, M. Takinoue, "Generation of monodisperse cell-sized microdroplets using a centrifuge-based axisymmetric co-flowing microfluidic device", *J. Biosci. Bioeng.* **119** (2015), no. 4, p. 492-495.

[10] M. Morita, H. Onoe, M. Yanagisawa, H. Ito, M. Ichikawa, K. Fujiwara, H. Saito, M. Takinoue, "Droplet-Shooting and Size-Filtration (DSSF) Method for Synthesis of Cell-Sized Liposomes with Controlled Lipid Compositions", *ChemBioChem* **16** (2015), no. 14, p. 2029-2035.

[11] S. Yasuda, M. Hayakawa, H. Onoe, M. Takinoue, "Generation of multi-helical microfibers and marble microbeads using orbital-rotation and axial-spin centrifuge", in *MicroTAS 2015 - 19th International Conference on Miniaturized Systems for Chemistry and Life Sciences*, Chemical and Biological Microsystems Society, 2015, p. 1163-1165.

[12] M. Morita, H. Yamashita, M. Hayakawa, H. Onoe, M. Takinoue, "Capillary-based centrifugal microfluidic device for size-controllable formation of monodisperse microdroplets", *J. Vis. Exp.* **2016** (2016), no. 108, article no. e53860.

[13] J. Sawayama, S. Takeuchi, "CORE-shell microparticles formation with centrifugal coaxial microfluidic device", in *2016 IEEE 29th International Conference on Micro Electro Mechanical Systems (MEMS)*, vol. 2016-Febru, Proceedings of the IEEE International Conference on Micro Electro Mechanical Systems (MEMS), no. January, IEEE, 2016, p. 708-709.

[14] S. Yasuda, M. Hayakawa, H. Onoe, M. Takinoue, "Twisting microfluidics in a planetary centrifuge", *Soft Matter* **13** (2017), no. 11, p. 2141-2147.

[15] Y. Morimoto, M. Onuki, S. Takeuchi, "Mass Production of Cell-Laden Calcium Alginate Particles with Centrifugal Force", *Advanced Healthcare Materials* **6** (2017), no. 13, article no. 1601375.

[16] J. A. De Lora, J. L. Velasquez, N. J. Carroll, J. P. Freyer, A. P. Shreve, "Centrifugal Generation of Droplet-Based 3D Cell Cultures", *SLAS Technol.* **25** (2020), no. 5, p. 436-445.

[17] Y. Cheng, X. Zhang, Y. Cao, C. Tian, Y. Li, M. Wang, Y. Zhao, G. Zhao, "Centrifugal microfluidics for ultra-rapid fabrication of versatile hydrogel microcarriers", *Applied Materials Today* **13** (2018), p. 116-125.

[18] J. Li, Y. Wang, L. Cai, L. Shang, Y. Zhao, "High-throughput generation of microgels in centrifugal multi-channel rotating system", *Chemical Engineering Journal* **427** (2022), article no. 130750.

[19] D. K. Boadi, A. Marmur, "Drop formation and detachment from rotating capillaries", *J. Colloid Interface Sci.* **140** (1990), no. 2, p. 507-524.

[20] K. Maeda, H. Onoe, M. Takinoue, S. Takeuchi, "Instantaneous solidification of a centrifuge-driven capillary jet with controlled hydrodynamic instability in a centrifuge-based droplet shooting device through observational analysis", in *Proceedings of the 16th International Conference on Miniaturized Systems for Chemistry and Life Sciences, MicroTAS 2012*, Chemical and Biological Microsystems Society, 2012, p. 878-880.

[21] K. Maeda, H. Onoe, M. Takinoue, S. Takeuchi, "Observation and manipulation of a capillary jet in a centrifuge-based droplet shooting device", *Micromachines* **6** (2015), no. 10, p. 1526-1533.

[22] H. B. Eral, E. R. Safai, B. Keshavarz, J. J. Kim, J. Lee, P. S. Doyle, "Governing Principles of Alginate Microparticle Synthesis with Centrifugal Forces", *Langmuir* **32** (2016), no. 28, p. 7198-7209.

[23] M. Badalan, G. Ghigliotti, J.-L. Achard, F. Bottausci, G. Balarac, "Physical Analysis of the Centrifugal Microencapsulation Process", *Ind. Eng. Chem. Res.* **61** (2022), no. 30, p. 10891-10914.

[24] W.-P. Voo, B.-B. Lee, A. Idris, A. Islam, B.-T. Tey, E.-S. Chan, "Production of ultra-high concentration calcium alginate beads with prolonged dissolution profile", *RSC Adv.* **5** (2015), no. 46, p. 36687-36695.

[25] S. V. Bhujbal, G. A. Paredes-Juarez, S. P. Niclou, P. de Vos, "Factors influencing the mechanical stability of alginate beads applicable for immunoisolation of mammalian cells", *J. Mech. Behav. Biomed. Mater.* **37** (2014), p. 196-208.

[26] E.-S. Chan, T.-K. Lim, W.-P. Voo, R. Pogaku, B. Ti Tey, Z. Zhang, "Effect of formulation of alginate beads on their mechanical behavior and stiffness", *Particuology* **9** (2011), p. 228-234.

[27] A. Martinsen, G. Skjåk-Bræk, O. Smidsrød, "Alginate as immobilization material: I. Correlation between chemical and physical properties of alginate gel beads", *Biotechnol. Bioeng.* **33** (1989), no. 1, p. 79-89.
[28] M. Peirone, C. J. D. Ross, G. Hortelano, J. L. Brash, P. L. Chang, "Encapsulation of various recombinant mammalian cell types in different alginate microcapsules", *J. Biomed. Mater. Res.* **42** (1998), no. 4, p. 587-596.
[29] A. Bartkowiak, D. Hunkeler, "Alginate-oligochitosan microcapsules: A mechanistic study relating membrane and capsule properties to reaction conditions", *Chem. Mater.* **11** (1999), no. 9, p. 2486-2492.
[30] V. Pillay, C. M. Dangor, T. Govender, K. R. Moopanar, N. Hurbans, "Drug release modulation from cross-linked calcium alginate microdiscs, 1: Evaluation of the concentration dependency of sodium alginate on drug entrapment capacity, morphology, and dissolution rate", *Drug Deliv.* **5** (1998), no. 1, p. 25-34.
[31] N. A. Hadjiev, B. G. Amsden, "An assessment of the ability of the obstruction-scaling model to estimate solute diffusion coefficients in hydrogels", *J. Control. Release* **199** (2015), p. 10-16.
[32] P. de Vos, A. Andersson, S. K. Tam, M. M. Faas, J. P. Hallé, "Advances and Barriers in Mammalian Cell Encapsulation for Treatment of Diabetes", *Immun., Endoc. & Metab. Agents in Med. Chem.* **6** (2006), p. 139-153.
[33] J. A. M. Steele, J. P. Hallé, D. Poncelet, R. J. Neufeld, "Therapeutic cell encapsulation techniques and applications in diabetes", *Advanced Drug Delivery Reviews* **67-68** (2014), p. 74-83.
[34] V. Iacovacci, L. Ricotti, A. Menciassi, P. Dario, "The bioartificial pancreas (BAP): Biological, chemical and engineering challenges", 2016, 12-27 pages.
[35] W. F. Kendall, M. D. Darrabie, H. M. El-Shewy, E. C. Opara, "Effect of alginate composition and purity on alginate microspheres", *J. Microencapsul.* **21** (2004), no. 8, p. 821-828.
[36] P. De Vos, A. F. Hamel, K. Tatarkiewicz, "Considerations for successful transplantation of encapsulated pancreatic islets", *Diabetologia* **45** (2002), no. 2, p. 159-173.
[37] Q. Deng, "Fluid dynamics study of bubble entrapment during encapsulation", PhD Thesis, Vanderbilt University, Nashville, USA, 2007, https://ir.vanderbilt.edu/handle/1803/10587, 159 pages.
[38] Q. Wang, S. Liu, H. Wang, J. Zhu, Y. Yang, "Alginate droplets pre-crosslinked in microchannels to prepare monodispersed spherical microgels", *Colloids Surf. A Physicochem. Eng. Asp.* **482** (2015), p. 371-377.
[39] B. F. Matlaga, L. P. Yasenchak, T. N. Salthouse, "Tissue response to implanted polymers: The significance of sample shape", *J. Biomed. Mater. Res.* **10** (1976), no. 3, p. 391-397.
[40] T. N. Salthouse, "Some aspects of macrophage behavior at the implant interface", *J. Biomed. Mater. Res.* **18** (1984), no. 4, p. 395-401.
[41] M. Spector, C. Cease, T.-L. Xia, "The local tissue response to biomaterials", *Critical Reviews in Biocompatibility* **5** (1989), no. 3, p. 269-295.
[42] E.-S. Chan, B.-B. Lee, P. Ravindra, D. Poncelet, "Prediction models for shape and size of ca-alginate macrobeads produced through extrusion-dripping method", *J. Colloid Interface Sci.* **338** (2009), no. 1, p. 63-72.
[43] M. Badalan, F. Bottausci, G. Ghigliotti, J.-L. Achard, G. Balarac, "Effects of process parameters on capsule size and shape in the centrifugal encapsulation technology: Parametric study dataset", *Data in Brief* **41** (2022), article no. 107851.
[44] G. I. Taylor, "The formation of emulsions in definable fields of flow", *Proc. R. Soc. Lond., Ser. A* **146** (1934), no. 858, p. 501-523.
[45] A. Luciani, M. F. Champagne, L. A. Utracki, "Interfacial tension coefficient from the retraction of ellipsoidal drops", *J. Polym. Sci. B Polym. Phys.* **35** (1997), no. 9, p. 1393-1403.
[46] J. Juza, "Surface Tension Measurements of Viscous Materials by Pendant Drop Method: Time Needed to Establish Equilibrium Shape", *Macromol. Symp.* **384** (2019), no. 1, article no. 1800150.
[47] B.-B. Lee, P. Ravindra, E.-S. Chan, "Size and shape of calcium alginate beads produced by extrusion dripping", *Chemical Engineering and Technology* **36** (2013), no. 10, p. 1627-1642.
[48] V. Y. Rivkind, G. M. Ryskin, "Flow structure in motion of a spherical drop in a fluid medium at intermediate Reynolds numbers", *Fluid Dynamics* **11** (1976), no. 1, p. 5-12.
[49] R. Yang, Q.-C. Lao, H.-P. Yu, Y. Zhang, H.-C. Liu, L. Luan, H.-M. Sun, C.-Q. Li, "Tween-80 and impurity induce anaphylactoid reaction in zebrafish", *J. Appl. Toxicol.* **35** (2015), no. 3, p. 295-301.
[50] J.-F. Guthmann, A. Karleskind, J.-P. Wolff, *Manuel des corps gras*, Technique et documentation Lavoisier, 1992, 1500 pages.
[51] F. Shahidi, *Bailey's Industrial Oil and Fat Products, Industrial and Nonedible Products from Oils and Fats*, 6^{th} ed., Bailey's Industrial Oil and Fat Products, vol. 6, John Wiley & Sons, 2005, 303-332 pages.
[52] B. D. Ribeiro, C. Florindo, L. C. Iff, M. A. Z. Coelho, I. M. Marrucho, "Menthol-based eutectic mixtures: Hydrophobic low viscosity solvents", *ACS Sustainable Chem. Eng.* **3** (2015), no. 10, p. 2469-2477.
[53] E. E. Franco, J. C. Adamowski, R. T. Higuti, F. Buiochi, "Viscosity measurement of newtonian liquids using the complex reflection coefficient", *IEEE Trans. Ultrason. Ferroelectr. Freq. Control.* **55** (2008), no. 10, p. 2247-2253.
[54] H. Nezammahalleh, M. Nosrati, F. Ghanati, S. A. Shojaosadati, "Exergy-based screening of biocompatible solvents for in situ lipid extraction from Chlorella vulgaris", *J. Appl. Phycol.* **29** (2017), no. 1, p. 89-103.

[55] K. Haldar, S. Chakraborty, "Effect of liquid pool concentration on chemically reactive drop impact gelation process", *J. Colloid Interface Sci.* **528** (2018), p. 156-165.

[56] L. Capretto, S. Mazzitelli, C. Balestra, A. Tosi, C. Nastruzzi, "Effect of the gelation process on the production of alginate microbeads by microfluidic chip technology", *Lab Chip* **8** (2008), no. 4, p. 617-621.

[57] T. D. Dang, S. W. Joo, "Preparation of tadpole-shaped calcium alginate microparticles with sphericity control", *Colloids and Surfaces B: Biointerfaces* **102** (2013), p. 766-771.

[58] Y. S. Lin, C. H. Yang, Y. Y. Hsu, C. L. Hsieh, "Microfluidic synthesis of tail-shaped alginate microparticles using slow sedimentation", *Electrophoresis* **34** (2013), no. 3, p. 425-431.

[59] Y. Hu, Q. Wang, J. Wang, J. Zhu, H. Wang, Y. Yang, "Shape controllable microgel particles prepared by microfluidic combining external ionic crosslinking", *Biomicrofluidics* **6** (2012), no. 2, article no. 026502.

[60] M. Cohen, L. E. J. Gladney, L. W. Kahn, *Classical Mechanics: a Critical Introduction*, first ed., Hindawi Publishing Corporation, 2011.